SUPERCOMPUTER SIMULATION OF RADIATIVE TRANSFER IN MULTIFRACTAL CLOUD MODELS[1]

Anthony Davis[2]
Atmospheric Environment Service
Dorval, Québec, Canada

Shaun Lovejoy
McGill University
Montréal, Québec, Canada

Daniel Schertzer
Laboratoire de Météorologie Dynamique
Paris, 5e, France

ABSTRACT

We numerically solve the solar transfer problem in an extremely variable lognormal multifractal medium for an isotropic conservative discrete angle phase function. Many features of the resulting radiation fields compare favorably with their real world counterparts. Most interestingly, we find that homogeneous appearance (weakly variable radiation fields) in no way guarantees homogeneous internal structure. Worse still, the bulk properties of the most homogeneous looking clouds are the most different from the plane-parallel prediction.

1. MOTIVATION AND OVERVIEW

Cloud structure is intimately related to the turbulent dynamics of the lower atmosphere. Recent advances in our understanding of turbulence are largely based on the concept of scale invariance: power law energy spectra, fractal and multifractal models of intermittency, etc. Moreover, scaling behavior is observed over a large range of scales for many atmospheric quantities, including cloud liquid water content (LWC) (e.g., King *et al.*, 1981; Duroure and Guillemet, 1990; Marshak *et al.*, 1993) as well as VIS/IR radiances (see Lovejoy (1982) and Gabriel *et al.* (1988) respectively for the first simple- and multiple-scaling studies). Breaks in scaling and multiple scaling regimes have also been reported (e.g., Cahalan and Joseph, 1989) but, for the purposes of pioneering radiative transfer investigations, we are inclined to use the simplest possible scaling cloud models that capture some degree of realism. For the present exercise we settle on a series of highly variable cloud models based on a specific realization of a discrete multifractal cascade with lognormal weights. Using the most robust numerical approaches to model the multiple scattering processes, we primarily study the solar problem (external illumination and conservative scattering) for which we have obtained the fully resolved reflected, transmitted, as well as internal radiation fields.

In the following section, we describe the adopted LWC field as well as the vast class of stochastic models it belongs to. In sect. 3, we briefly review the type of Discrete Angle (DA) radiative transfer which we use for conceptual and computational simplicity. We present and discuss some of our results in sect. 4 before concluding and pointing out some possible implications, mainly in connection with radiation parameterization schemes in climate forecasting using GCMs and NWP.

2. THE ADOPTED MULTIFRACTAL CLOUD (EXTINCTION FIELD)

At such an early stage in the development of our understanding of radiative transfer in inhomogeneous optical media, it is entirely justifiable to work in the smallest possible dimensionality where variability effects still occur; this seems to be 2D. We will first describe algorithmically, then mathematically and graphically our prototypical density field, equivalently, the LWC distribution $\rho(\mathbf{x})$ where $\mathbf{x} = (y,z)^T \in [0,L]^2$, where L is the "outer" scale of the cloud (superscript "T" means transpose).

In order to generate $\rho(y,z)$, we use one of the simplest possible models that emulates the turbulent break-up of eddies into sub-eddies: a multiplicative cascade. Starting with $\rho(y,z) = 1$ everywhere on $[0,L]^2$, we divide this square domain into $\lambda_0^2 = 4$ sub-domains where the density is multiplied by 4 independent positive random weights $W = \lambda_0^{\gamma}$ of unit average ($\langle W \rangle = 1$). We used lognormal deviates: γ, the random "generator," is drawn from a normal distribution with variance σ^2 (that we will denote $2C_1 \ln\lambda_0$ for future convenience, with $C_1 = 0.5$). The mean $\langle\gamma\rangle$ is taken to be $-\sigma^2/2$, this choice enforces the multifractal "conservation" constraint ($\langle\lambda_0^{\gamma}\rangle = 1$). The whole procedure is recursively iterated n = 10 times so we end up with a 2D grid with

$$\lambda = L/l_0 = \lambda_0^{\,n} \tag{0}$$

i.e., 1024 cells on a side, and we denote the corresponding density field ρ_λ; l_0 is the grid constant or "inner" scale of the cloud.

Summarizing, we see that every final density value can be written as

$$\rho_\lambda = \prod_{i=1}^{n} \lambda_0^{\gamma_i} \tag{1}$$

with $\lambda_0 = 2$ (for simplicity) and n = 10 (in order to have a large range of scales at our disposal, $\lambda \gg 1$). The p.d.f. of ρ_λ is given by

$$\mathrm{Prob}\{\lambda^{\gamma} \le \rho_\lambda < \lambda^{\gamma+d\gamma}\} \sim \lambda^{-c_\rho(\gamma)}d\gamma \tag{2}$$

where "~" means that we can neglect terms in $\ln\lambda$ and where

$$c_\rho(\gamma) = \frac{C_1}{4}\left(\frac{\gamma}{C_1} + 1\right)^2 \tag{3}$$

In going from (0-1) to (2-3), one can use the additive properties of Gaussian r.v.'s (i.e., means and variances add). The above-mentioned value of $C_1 = 0.5$ is close to that determined from the "intermittency correction" deduced from King *et al.*'s (*ibid.*) LWC power spectra; see Davis *et al.* (1991a) for full details. It is important to note that eq. (2) is generic to all multifractal fields and, in essence, $c_\rho(\gamma)$ is a scale invariant characterization of ρ_λ's histogram; in contrast, eq. (3) is specific to the lognormal model and many other examples can be found in the multifractal literature (see, e.g., Schertzer and Lovejoy, 1987).

Figures 1a,b,c illustrate the extreme variability of the final density field $\rho_\lambda(y,z)$ by showing the "exceedence sets," respectively for thresholds $\lambda^{-C_1} = 1/32$ (i.e., the event that $\gamma \ge -C_1$), $\lambda^0 = 1$ ($\gamma \ge 0$), $\lambda^{C_1} = 32$ ($\gamma \ge C_1$). In our specific realization, we find a spatial average $\overline{\rho_\lambda} \approx 1.52$ while $\min\{\rho_\lambda\} \approx 10^{-6.7}$ and $\max\{\rho_\lambda\} \approx 10^{4.1}$. Notice the concentration of mass in the lower l.h.s. of the medium. Notice also how the notion of (smooth) level "curve" fails totally for such distributions and how very sparse the two latter sets are. Their fractal dimensions $D(\gamma)$ are defined by the number of cells ("boxes") at relative scale ("resolution") $1/\lambda$ needed to cover them; namely,

$$N\{\rho_\lambda \ge \lambda^{\gamma}\} \sim \lambda^{D_\rho(\gamma)} \tag{4}$$

Multiplying eq. (2) by the total number of cells λ^d (d=2 is the dimension of space) and integrating from γ to ∞, we find

$$D_\rho(\gamma) = d - c_\rho(\gamma) \tag{5}$$

as long as $c_\rho(\gamma)$ is non-decreasing on $[\gamma,\infty[$. (In the $\lambda \gg 1$ limit, the integral will be dominated be the contribution from the lower bound and, furthermore, we can neglect all terms in $\ln\lambda$ that may occur.) From (5), we can see why $c(\gamma)$ is called the "codimension function" while γ is called the "order of singularity" since $\rho_\lambda \to \infty$ as $\lambda \to \infty$ if $\gamma > 0$ (and $\gamma < 0$ yields in fact a "regularity" since then $\rho_\lambda \to 0$). Finally, ρ_λ is called a "multifractal" since an infinite number of fractal dimensions are needed to describe it (Frisch and Parisi, 1985). For the sets in figs. 1a,b,c, eqs. (3–5) yield $D_\rho(-C_1) = d = 2$ (this set fills space), $D_\rho(0) = 1.875$, and $D_\rho(C_1) = 1.5$; for the meanings of these values of γ with respect to the statistical moments $\langle\rho_\lambda^q\rangle$ ($q = 0, 1/2, 1$), see Davis (1992).

[1]Supported by DoE's ARM program (contract #DE-FG03-90ER61062).
[2]Now at NASA/GSFC (Code 913), Greenbelt, MD 20771, USA.

ISBN 0-937194-28-X

Now density $\rho(y,z)$—scattering particles per unit of 2D "volume"—is simply related to extinction—probability of photon/particle interaction per unit of length—that we will denote in Chandrasekhar (1960) fashion as $\kappa\rho(y,z)$, where κ—2D cross-"section" per particle—is taken to be uniform over the entire domain. Quantitatively, we determine κ in such a way that the average optical thickness of the entire cloud ($\langle\tau\rangle = \kappa\langle\rho_\lambda\rangle L$ where $\langle\rho_\lambda\rangle = 1$, by conservation) is $\gg 1$, while its counterpart for the individual cells ($\langle\tau_0\rangle = \kappa\langle\rho_\lambda\rangle l_0$) is still $\ll 1$. In the computationally convenient units where $l_0 = 1$ (hence $L = \lambda = 2^{10}$), κ can take such values as $2^{-7},\ldots,2^{-3}$, yielding $\overline{\tau} \approx 12.2,\ldots,195$ (by factors of 2). So we have five distinct cloud thicknesses to consider.

3. COMPUTATIONAL DA RADIATIVE TRANSFER IN 2D

For the sake of simplicity, we will perform *bone fide* 2D transfer, not 3D transfer with no variability along the x-axis as, e.g., in Evans (1993). The corresponding radiance field $I(y,z;\theta)$ obeys the following transfer equation

$$\left\{\sin\theta\frac{\partial}{\partial y} + \cos\theta\frac{\partial}{\partial z} - \kappa\rho(y,z)\int_{-\pi}^{+\pi}[p(\theta'\rightarrow\theta)\text{-}\delta(\theta'\text{-}\theta)]\,[\cdot]\,d\theta\right\}I(y,z;\theta) = 0 \tag{6}$$

where $\theta\in\,]-\pi,+\pi]$ is measured away from the (downward oriented) z-axis. We now make the (orthogonal beam) DA assumption that

$$I(y,z;\theta) = I_{+z}(y,z)\delta(\theta) + I_{-z}(y,z)\delta(\theta-\pi) + I_{+y}(y,z)\delta(\theta-\frac{\pi}{2}) + I_{-y}(y,z)\delta(\theta+\frac{\pi}{2}) \tag{7}$$

and, accordingly, $p(\theta'\rightarrow\theta)$ becomes, for "relative angle" scattering,

$$p(\theta'-\theta) = f\delta(\theta'-\theta) + b\delta(\theta'-\theta-\pi) + s[\delta(\theta'-\theta-\frac{\pi}{2}) + \delta(\theta'-\theta+\frac{\pi}{2})] \tag{8}$$

The first three harmonics determine this DA phase function entirely:

$\varpi_0 = f + b + 2s$	single scattering albedo	(9a)
$\varpi_1 = \varpi_0 g = f - b$	asymmetry factor (g)	(9b)
$\varpi_2 = f + b - 2s$	(no special name)	(9c)

In the following, we will look at isotropic ($\varpi_1 = \varpi_2 = 0$) scattering, hence for $f = b = s = \varpi_0/4$, mainly in the conservative ($\varpi_0 = 1$) case. Lovejoy *et al.* (1990), Gabriel *et al.* (1990), and Davis *et al.* (1990) show in various ways that DA scattering kernels are acceptable surrogates for their continuous angle (CA) counterparts, at least if we are concerned only with scaling of bulk radiative properties with range of scales and/or optical mass since structural- and not optical aspects dominate the picture.

After defining a formal DA radiance 4-vector substitution of (7–8) into the integro-differential transfer eq. (6) yields the following finite system of equations for multiple DA scattering:

$$\left\{\begin{pmatrix}1&0&0&0\\0&-1&0&0\\0&0&0&0\\0&0&0&0\end{pmatrix}\frac{\partial}{\partial y} + \begin{pmatrix}0&0&0&0\\0&0&0&0\\0&0&1&0\\0&0&0&-1\end{pmatrix}\frac{\partial}{\partial z} - \kappa\rho(y,z)\begin{pmatrix}f\text{-}1&b&s&s\\b&f\text{-}1&s&s\\s&s&f\text{-}1&b\\s&s&b&f\text{-}1\end{pmatrix}\right\}\begin{pmatrix}I_{+y}\\I_{-y}\\I_{+z}\\I_{-z}\end{pmatrix} = 0 \tag{10}$$

Notice that the DA "radiances" that appear in (7) and (10) in fact have units of flux. Finally, boundary conditions (BCs) for the solar (or "albedo") problem with horizontally cyclical replication of the given density field are

$$I_{+z}(y,0) = 1,\ I_{-z}(y,L) = 0 \quad \text{for } y\in[0,L[\tag{11a}$$
$$I_{\pm y}(L,z) = I_{\pm y}(0,z) \quad \text{for } z\in\,]0,L[\tag{11b}$$

where z=0 corresponds to the top in fig. 1. Eqs. (10, 11a,b) with the multifractal $\rho(y,z)$ described in section 2 define a highly non-trivial computational transfer problem, mainly due to the occurrence of very thick cells: already at $\log_2\kappa = -7$, $\max\{\tau_0\} \approx 10^2$! The problem was solved in two completely independent ways for the thinnest cloud and good agreement was obtained. We adopted the two most brute-force methodologies (and paid the computational price in CPU-time): direct Monte Carlo simulation and straightforward relaxation of the spatially discretized version of (10). Because of the very thick cells, the latter technique called for tabulated single-cell coefficients, not the usual implicit or explicit linearization; see Davis (1992) for further details, including a brief discussion of performance, and Evans (*ibid.*) for a promising CA approach based on spherical harmonics. The thicker clouds were treated only by the Monte Carlo procedure which, incidentally, can be considerably optimized in DA transfer, far beyond standard variance reduction techniques.

4. RESULTS AND DISCUSSION

Rather than the $I_{\pm i}$ (i=y,z) themselves, it is of interest to consider the DA radiance vector in its scattering/extinction matrix' eigenvector representation (which is the DA equivalent of spherical harmonics). The last matrix that appears in (10) has the following eigenvalues and -vectors:

$1-\varpi_0$,	$J = I_{+y} + I_{-y} + I_{+z} + I_{-z}$	Total DA "Radiance"	(12a)
$1-\varpi_1$,	$\mathbf{F} = (I_{+y}\text{-}I_{-y}, I_{+z}\text{-}I_{-z})^T$	Net Flux Vector	(12b)
$1-\varpi_2$,	$K = -[I_{+y} + I_{-y}] + [I_{+z} + I_{-z}]$	"Non-Diffusive" Component	(12c)

Notice how they map directly onto the harmonic representation of the phase function in eqs. (9a,b,c). The name chosen for K is justified by the fact that, when it vanishes identically, (10) is equivalent to a diffusion law for J associated with a Fickian constitutive relation for **F** (Davis *et al.*, 1991b). In particular, we will require in the following the albedo and transmittance fields, namely,

$$R(y) = 1\text{-}F_z(y,0) = I_{-z}(y,0),\ T(y) = F_z(y,L) = I_{+z}(y,L) \text{ for } y\in[0,L[\tag{13}$$

Fig. 2 gives the bulk transmittance of the cloud as a function of $\overline{\tau}$, computed in three different ways: (i) assuming homogeneity yields the lowest value, the closed-form plane-parallel result $T_{pp}(\overline{\tau}) = 1/(1+b\overline{\tau})$; (ii) assuming "independent pixels" (IPs), an expression of Cahalan's (1989), viz. $T_{ip} = T_{pp}(\tau)$ where $\tau(y)$ is the colomn-wise local optical thickness—this also corresponds to s = 0 in eqs. (8–12); (iii) the numerical result $T = T(y)$. We notice in passing that $T\text{-}T_{pp}(\overline{\tau})$ generously spans the range of systematic discrepancies between observed and homogeneously computed fluxes reported in the literature (e.g., Wiscombe *et al.*'s (1984) discussion of the cloud "albedo paradox"). Clearly,

$$T_{ip} > T_{pp} \tag{14a}$$

is a direct consequence of Jensen's integral inequality (Hardy *et al.*, 1952) applied to the averaging of the convex function $T_{pp}(\overline{\tau})$. The inequality

$$T > T_{ip} \tag{14b}$$

is more interesting and is likely to generalize to CAs but only for the most θ-symmetrical illumination conditions (e.g., normal if collimated). Using first principles, Davis (1992) relates (14b) to a very general mechanism of inhomogeneous radiation transport known as "channeling" (Cannon, 1970) in the astrophysical literature.

The net flux vector $\mathbf{F}(\mathbf{x})$ is divergence-free by conservation of radiant energy. Consequently, flux-lines neither start nor stop inside the medium but at the upper and lower boundaries respectively. Naturally enough, the lines are repelled by dense regions and concentrate in tenuous ones, as illustrated in fig. 3. Channeling is directly traceable to the nonlinear coupling of the radiation- and density- (or extinction-) fields by the equations of transfer and the optically thicker the cloud, the stronger the nonlinearities. In extremely variable, highly correlated media such as multifractals, channeling will lead to the strong systematic effects observed in the bulk responses but, most interestingly, it is mediated by net horizontal fluxes that are of relatively small magnitude in comparison with their vertical counterparts according to our simulations (thin cloud standard deviation ≈15% of $T=\overline{F_z}$). *In situ* measurement of these horizontal fluxes in real cloud will be a challenge but this seems to be a prerequisite if we want to determine the role of channeling in the atmosphere.

Our Monte Carlo approach naturally yields order-of-scattering decompositions of the bulk responses: cumulative $T^{(n)}$ and $1\text{-}R^{(n)}$ which are plotted as a function of $\log_2 n$ in figs. 4a,b for the thinnest and thickest clouds along with their plane-parallel counterparts. We notice that the typical multiplicity of the multifractal's exiting radiation is smaller than the homogeneous medium of equal optical mass. This allows us to anticipate weaker absorption due to the cloud's LW alone in situations where $\varpi_0<1$. However, the smaller n-values are traceable to systematically enhanced geometrical photon paths (Davis, 1992) which, in turn, will promote absorption by the well-mixed (homogeneously distributed) gaseous species, including water vapor. Which will be the net outcome is unclear for the moment and the answer will of course depend on the model. These questions are clearly of importance to the cloud "absorption anomaly" problem in the solar IR (Stephens and Tsay, 1990).

Fig. 5a illustrates R(y) and T(y) for $\overline{\tau}=12.2$ and in fig. 5b we find the associated "apparent" absorptance field A(y)=1-R(y)-T(y). The range of A(y) is comparable to that of the observed values compiled by Fouquart *et al.* (1990)—expect for the most negative fluctuations (apparent "sources" embedded in the cloud) but this may however be due to the rejection of values viewed as unrealistic, too "unphysical" (Y. Fouquart, p.c.). Our average A(y) is of course zero, by conservation, and its true meaning is the (column-integrated) divergence of the horizontal flux:

$$[1\text{-}R(y)] - [T(y)\text{-}0] = F_z(y,z)\Big|_{z=L}^{z=0} = -\int_0^L\frac{\partial F_z}{\partial z}dz = \int_0^L\frac{\partial F_y}{\partial y}dz \tag{15}$$

where the last step makes use of radiant energy conservation ($\nabla\cdot\mathbf{F}=0$). In Stephens' (1986) usage of horizontal Fourier transforms in heterogeneous transfer, a "pseudo-source/sink" radiance term, closely related to $\partial F/\partial y$, naturally appears, siding with extinction, (true) absorption and scattering.

Fig. 6 illustrates, in scale invariant fashion, the variability of the five albedo fields, i.e., interpreting eq. (2) as an operational definition of $c_R(\gamma)$ for R(y)/R (which, like ρ_λ, is of unit average) for the five media. We see the gradual narrowing of the singularity spectrum—the field looks more and more homogeneous—as the cloud thickens ... and behaves less homogeneously (cf. fig. 2)! Clearly, both the powerful R(y)-smoothing and the signature of inhomogeneity in R (or 1-T) are boosted by the enhanced multiplicity of the scattered radiation in the denser clouds (figs. 4a,b); the apparent smoothness results directly from the longer photon free paths. Incidentally, the $c_R(\gamma)$'s in fig. 6 are remarkably similar to those obtained by Gabriel *et al.* (1988), given that they study the cumulative distribution of VIS radiances from GOES, i.e., they obtain only the ascending branch of $c_R(\gamma)$, as in eqs. (4-5).

The internal radiation fields were also obtained but for the extreme values of κ only. We refer the reader to Davis *et al.* (*ibid.*) for gray-scale renderings of both complete collections of the DA radiation fields as well as the density (in fact order of singularity) field. Complete statistical analyses of the compiled database are under way and will be published elsewhere. The most spectacular feature of the radiation fields is the strong degree of anisotropy which is partly due the up/down asymmetric BCs in (11a), partly due to the persistence of the underlying grid structure in the discrete cascade, and partly due to a fundamental mathematical aspect of transfer (somewhat enhanced by the simplistic DA model): we are dealing with directional derivatives. The J-fields are apparently the only ones affected by the former and quite natural cause. The second cause is artificial and affects all the fields but can, in principle be avoided by using CA transfer and continuous (Schertzer and Lovejoy, 1987) cascades. Fig. 7 illustrates the last and most interesting cause with the spatially averaged power spectra of F_z in both y- and z-directions which unsurprisingly scale very well. More precisely, we have plotted

$$\overline{F_z}(k_y) = \frac{1}{L}\int_0^L F_z(k_y,z)\,dz,\ \overline{F_z}(k_z) = \frac{1}{L}\int_0^L F_z(y,k_z)\,dy \qquad (16)$$

where k_i (i=y,z) is the corresponding wavenumber. The exponents are slightly greater than -1 and -2, i.e., respectively similar to "flicker noise" and "Brownian motion." Notice that the DA transfer eq. (10) constrains $\partial F_z/\partial z$ (and its opposite, $\partial F_y/\partial y$) but not $\partial F_z/\partial y$ (nor $\partial F_y/\partial z$). In more statistical terms, we expect $F_z(y,z)$ to have small (and apparently stationary) increments along the z-axis, not necessarily along the y-axis (it can be arbitrarily irregular). Fig. 7 also underscores yet another realistic aspect of our simulations since the (upper) $\overline{F_z}(k_y)$ curve is representative of (but less noisy than) the power-spectrum of R(y) and that a vast majority of the published spectra of remotely sensed albedo fields show scaling with exponents close to -1 (see, e.g., Cahalan and Snider, 1989).

Unsurprisingly, a joint examination of the convergence/divergence patterns of the (anisotropic but apparently stationary) F_y-, F_z-, and associated ρ-fields shows evidence of large and small scale channeling events, as sketched in fig. 3. K-fields are rarely small in the thin cloud rarely large in the thick one, i.e., the diffusion approximation will be poor in the former case (more akin to broken cloud) more accurate in the latter case (more akin to a stratus situation). This last finding is in agreement with the *in situ* observations of King *et al.* (1990) that show the radiance field to be diffusion-like deep inside real (marine StCu) cloud decks. However, these authors measure only the vertical component of **F** (for purely instrumental reasons) and the IP approximation they apply to reduce their data to obtain cloud optical thicknesses is therefore not totally justified and is likely to lead to systematic biases.

5. CONCLUSIONS AND IMPLICATIONS

Having performed extensive numerical simulations of radiative transfer in a typical multifractal cloud, we find it to share many radiative features with clouds in Nature. In particular, we find that the power- and singularity spectra of the albedo field compare favorably with those observed from satellite VIS channel imagery of cloudy scenes. The same can be said of the range found for the "apparent" absorption fields. Using Preisendorfer's (1976) jargon, we also find that the most apparently homogeneous models are those that exhibit the greatest differences in overall (domain-averaged) response when compared to their inherently homogeneous counterparts; such differences between observed and homogeneously calculated fluxes have been discussed at length in the literature. Moreover, since all current GCM radiation parameterizations assume homogeneity within the cloudy "fraction" of each cell/level, systematically wrong estimates of the radiative budgets can be expected.

The internal and exiting radiative flux fields show strong evidence of "channeling," the basic inhomogeneous transport mechanism that we hold as responsible for the systematic effects observed in the bulk properties. Closely related is the severe perturbation that we find in the order-of-scattering make-up of the cloud's responses. The information on the multiplicity of the scattering will allow us to anticipate inhomogeneity effects in the cloud's (true) absorption properties and, if these last effects prove to be strong and systematic, then GCM radiative heating rates will also be off-target. Finally, we further our argument that, in general, diffusion theory in multifractal clouds is best viewed as an interesting transport problem in its own right rather than a valid approximation to radiative transfer; to what extent this carries over to real clouds is an important question for future research.

ACKNOWLEDGMENTS

We thank R. Borde, R. Davies, C. Gauthier, D. Lavallée, P. Silas, and Y. Tessier, as well as R. Cahalan, A. Marshak, W. Ridgeway, and W. Wiscombe for many a fruitful discussion. We are grateful to *Météo-France* for many a CPU-hour on the *C²VR* 's Cray-2.

REFERENCES

Cahalan, R.F., 1989: Overview of Fractal Clouds. In *Advances in Remote Sensing (RSRM'87)*, A. Deepak *et al.* (Eds.), Deepak Publ., 371–389.

Cahalan, R. F., and J. H. Joseph, 1989: Fractal Statistics of Cloud Fields, *Mon. Wea. Rev.*, **117**, 261–272.

Cahalan, R. F., and J. B. Snider, 1989: Marine Stratocumulus Structure, *Remote Sens. Environ.*, **28**, 95–107.

Cannon, C. J., 1970: Line Transfer in Two Dimensions, *Ap. J.*, **161**, 255-264.

Chandrasekhar, S., *Radiative Transfer*, Dover, New York, NY, 1960.

Davis, A. B., P. Gabriel, S. Lovejoy, D. Schertzer, and G. L. Austin, 1990: Discrete Angle Radiative Transfer - Part III: Numerical Results and Atmospheric Applications, *J. Geophys. Res.*, **95**, 11729-11742.

Davis, A. B., S. Lovejoy, and D. Schertzer, 1991a: Radiative Transfer in Multifractal Clouds. In *Scaling, Fractals and Non-Linear Variability in Geophysics*, D. Schertzer and S. Lovejoy (Eds.), Kluwer, 303–318.

Davis, A., S. Lovejoy, and D. Schertzer, 1991b: Discrete Angle Radiative Transfer in a Multifractal Medium, *S.P.I.E. Proc.*, **1558**, 37–59.

Davis, A. B., 1992: *Radiation Transport in Scale Invariant Optical Media*, Ph.D. thesis, Physics Dpt., McGill Un., Montréal (Qc.), Canada, xviii+332 pp.

Duroure, C., and B. Guillemet, 1990: Analyse des Hététrogenéités Spatiales des Stratocumulus et Cumulus, *Atmos. Res.*, **25**, 331-350.

Evans, K. F., 1993: Two-dimensional Radiative Transfer in Cloudy Atmospheres - Part 1, The Spherical Harmonic Spatial Grid Method, accepted by *J. Atmos. Sci.*

Fouquart, Y., J. C. Buriez, M. Herman, and R. S. Kandel, 1990: The Influence of Clouds on Radiation - A Climate Modeling Perspective, *Rev. of Geophys.*, **28**, 145–166.

Frisch, U., and G. Parisi, 1985: A Multifractal Model of Intermittancy, in *Turbulence and Predicability in Geophysical Fluid Dynamics and Climate Dynamics*, M. Ghil, R. Benzi, and G. Parisi (Eds.), North-Holland, 84–88.

Gabriel, P., S. Lovejoy, D. Schertzer, and G. L. Austin, 1988: Multifractal Analysis of Resolution Dependence in Satellite Imagery, *Geophys. Res. Lett.*, **15**, 1373–1376.

Gabriel, P., S. Lovejoy, A. B. Davis, D. Schertzer, and G. L. Austin, 1990: Discrete Angle Radiative Transfer - Part II: Renormalization Approach for Homogeneous and Fractal Clouds, *J. Geophys. Res.*, **95**, 11717-11728.

Hardy, G. H., J. E. Littlewood, and G. Pólya, 1952: *Inequalities*, Cambridge University Press, 2nd ed.

King, M. D., L. F. Radke, and P. V. Hobbs, 1990: Determination of the Spectral Absorption of Solar Radiation by Marine Stratocumulus Clouds from Airborne Measurements Within Clouds, *J. Atmos. Sci.*, **47**, 894-907.

King, W. D., C. T. Maher, G. A. Hepburn, 1981: Further Performance Tests on the CSIRO Liquid Water Probe, *J. Atmos. Sci.*, **38**, 195-200.

Lovejoy, S., 1982: The Area-Perimeter Relation for Rain and Clouds, *Science*, **216**, 185–187.

Lovejoy, S., A. B. Davis, P. Gabriel, D. Schertzer, and G. L. Austin, 1990: Discrete Angle Radiative Transfer - Part I: Scaling and Similarity, Universality and Diffusion, *J. Geophys. Res.*, **95**, 11699-11715.

Marshak, A., W. Wiscombe, and A. B. Davis, 1993: On the Analysis of the Multifractal Properties of Cloud Liquid Water Data. In *IRS'92: Current Problems in Atmospheric Radiation*, S. Keevallik (Ed.), Deepak Publ., Hampton (Va.), this volume.

Schertzer, D., and S. Lovejoy, 1987: Physically Based Rain and Cloud Modeling by Anisotropic, Multiplicative Turbulent Cascades, *J. Geophys. Res.*, **92**, 9693–9714.

Stephens, G. L., 1986: Radiative Transfer in Spatially Heterogeneous, Two-Dimensional Anisotropically Scattering Media, *J. Quant. Spectrosc. Radiat. Transfer*, **36**, 51–67.

Stephens, G. L., and S.-C. Tsay, 1990: On the Cloud Absorption Anomaly, *Q. J. R. Meteorol. Soc.*, **116**, 671-704.

Preisendorfer, R. W., 1976: *Hydrological Optics*, vols. 1-2, NOAA/PMEL.

Wiscombe, W. J., R. M. Welch, and W. D. Hall, 1984: The Effects of Very Large Drops on Cloud Absorption - Part 1, Parcel Models. *J. Atmos. Sci.*, **41**, 1336-1355.

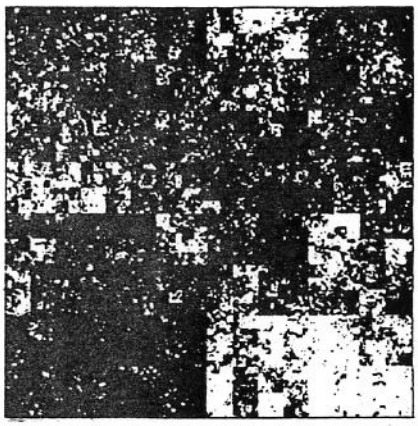

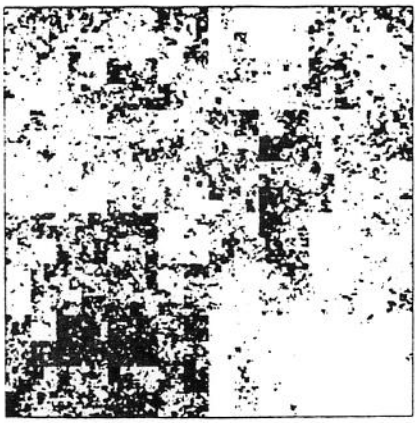

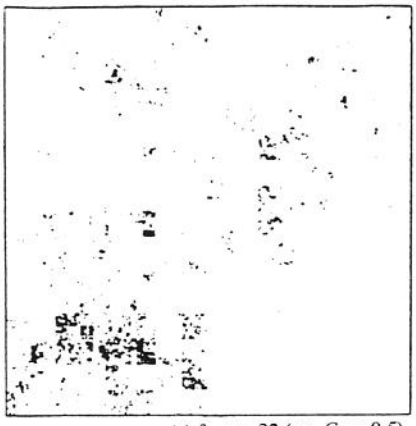

Fig. 1. Cloud model exceedence sets: (a) for $\rho \geq 1/32$ ($\gamma \geq -C_1 = -0.5$), (b) for $\rho \geq 1$ ($\gamma \geq 0$), (c) for $\rho \geq 32$ ($\gamma \geq C_1 = 0.5$).

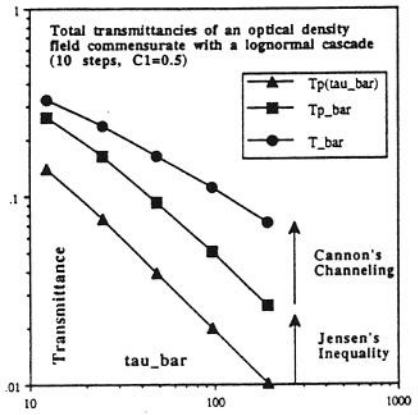

Fig. 2. Comparison of three different ways of estimating the bulk DA transmittance for the five clouds: computational 2D transfer, semi-analytical "IP" averaging, analytical plane-parallel theory.

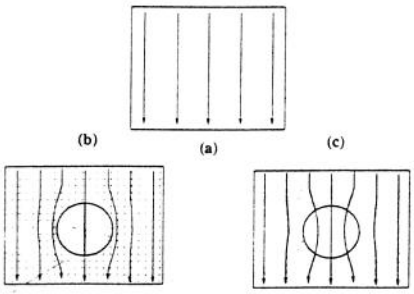

Fig. 3. Schematic for radiative "channeling:" (a) unperturbed fields, (b) around a dense region, (c) through a tenuous one. Notice the increased number of flux-lines (hence total transmittance) in both cases; this applies to the case of constant total mass (Davis, 1990).

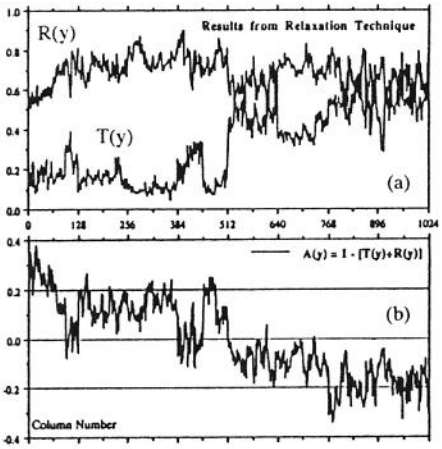

Fig. 5. (a) the albedo R(y) and transmittance T(y) fields for $\kappa=2^{-7}$, and (b) apparent absorptance A(y) = 1-[R(y)+T(y)].

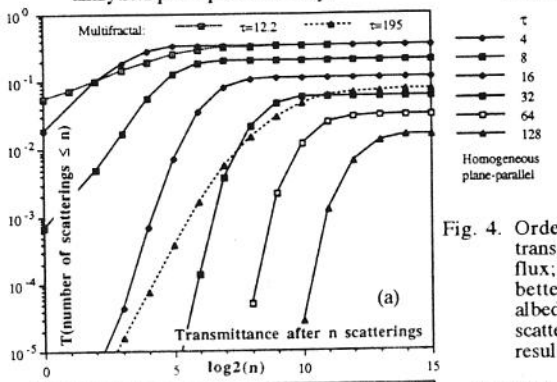

Fig. 4. Orders of DA scattering: (a) for transmitted- and, (b) for non-reflected flux; the latter choice of representation better illustrates scaling regime for albedo. Calculations for isotropic CA scattering yield almost indistinguishable results.

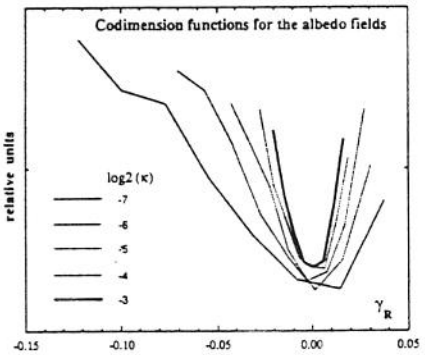

Fig. 6. Singularity spectra for the albedo fields.

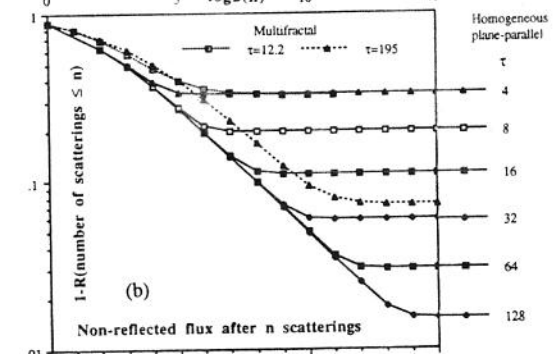

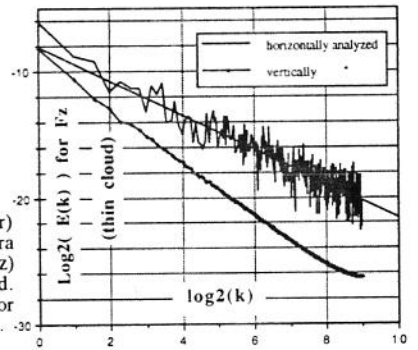

Fig. 7. Average horizontal (upper) and vertical (lower) spectra for the vertical flux $F_Z(y,z)$ through the thin cloud. Similar results are found for F_Y and for the thick cloud.